Isolation of Retinal Arterioles for *Ex Vivo* Cell Physiology Studies

Tim M. Curtis*[1], Declan McLaughlin[2], Michael O'Hare[1], Joanna Kur[1], Peter Barabas[1], Gordon Revolta[1], C. Norman Scholfield[3], J. Graham McGeown[4], Mary K. McGahon*[2]

[1]Centre for Experimental Medicine, Queen's University of Belfast

[2]Centre for Biomedical Sciences (Education), Queen's University of Belfast

[3]Department of Pharmaceutical Chemistry and Pharmacognosy, Naresuan University

[4]School of Medicine, Dentistry and Biomedical Sciences, Queen's University of Belfast

*These authors contributed equally

Correspondence to: Mary K. McGahon at m.mcgahon@qub.ac.uk

Abstract

The retina is a highly metabolically active tissue that requires a substantial blood supply. The retinal circulation supports the inner retina, while the choroidal vessels supply the photoreceptors. Alterations in retinal perfusion contribute to numerous sight-threatening disorders, including diabetic retinopathy, glaucoma and retinal branch vein occlusions. Understanding the molecular mechanisms involved in the control of blood flow through the retina and how these are altered during ocular disease could lead to the identification of new targets for the treatment of these conditions. Retinal arterioles are the main resistance vessels of the retina, and consequently, play a key role in regulating retinal hemodynamics through changes in luminal diameter. In recent years, we have developed methods for isolating arterioles from the rat retina which are suitable for a wide range of applications including cell physiology studies. This preparation has already begun to yield new insights into how blood flow is controlled in the retina and has allowed us to identify some of the key changes that occur during ocular disease. In this article, we describe methods for the isolation of rat retinal arterioles and include protocols for their use in patch-clamp electrophysiology, calcium imaging and pressure myography studies. These vessels are also amenable for use in PCR-, western blotting- and immunohistochemistry-based studies.

Video Link

The video component of this article can be found at https://www.jove.com/video/57944/

Introduction

Understanding how blood flow is controlled in the retina is an important goal, since abnormal blood flow has been implicated in the pathogenesis of a variety of sight-threatening retinal diseases[1,2,3,4]. The retinal circulation, which supplies the inner retinal neurons and glial cells, has an end artery arrangement, with all of the blood from the retinal arteries and arterioles passing through the capillaries to the retinal venules and finally veins[5]. Blood flow in the retina is regulated by the tone of the retinal arteries and arterioles as well as the contractile activity of the pericytes located on the walls of the retinal capillaries and post-capillary venules[6,7,8]. The control of retinal vascular tone is complex and is modulated by a range of inputs from the circulatory system and surrounding retinal tissue, including blood gases, circulating molecules and hormones, and vasoactive substances released from the retinal vascular endothelium and macroglia[9,10,11]. The retinal arterioles are the small arterial branches of the retina and are composed of a single layer of vascular smooth muscle cells and an inner lining of longitudinally arranged endothelial cells[12,13,14]. These vessels form the main site of vascular resistance within the retinal circulation and therefore play an important role in the local control of retinal blood flow. Retinal arterioles regulate capillary blood flow in the retina by dilating or constricting their luminal diameter, mediated by changes in vascular smooth muscle contractility[10,15,16]. Understanding the molecular mechanisms through which retinal arterioles regulate retinal perfusion therefore requires preparations where the arteriolar smooth muscle cells can be accessed and studied in conditions as close to physiological as possible.

Ex vivo preparations of isolated retinal blood vessels provide access to the vascular smooth muscle cells, whilst still retaining their functionality and interconnectivity with the underlying endothelium. Most studies to date using isolated vessels have focused on large bovine or porcine arterial vessels (60 - 150 µm). These can be mounted in commercially available wire or pressure myograph systems to enable pharmacological interrogation of vascular smooth muscle cell contractile mechanisms[17,18]. Such preparations have greatly contributed to our knowledge of retinal vascular physiology under normal conditions. Few studies have used retinal arterioles isolated from small laboratory animals as their smaller diameter (~ 8 - 45 µm) prevents their use in conventional myography systems[19,20,21,22]. An important advantage, however, of using vessels from small laboratory animals is the wide availability of genetically modified, transgenic and retinal disease models. Small laboratory animals are also more amenable for use in *in vivo* intervention studies.

Here we describe straightforward protocols for isolating and cannulating rat retinal arterioles for pressure myography experiments. Ca^{2+} imaging and electrophysiology protocols using these vessels are also detailed. These can provide further insights into the regulation of vascular smooth muscle contractility and blood flow in the retina.

Protocol

All experiments described here were performed in accordance with guidelines contained within the UK Animals (Scientific Procedures) Act of 1986 and were approved by the Queen's University of Belfast Animal Welfare and Ethical Review Body.

1. Isolation of Retinal Arterioles

Note: The following protocol is used to isolate retinal arterioles. This method is optimized for rat retinal arterioles but can be used with mouse retinas. The yield of vessels, however, is lower when using mice.

1. Make up a solution of low Ca^{2+} containing Hanks' (LCH) as shown in **Table 1**.
    NOTE: This solution can be stored for up to 3 days at 4 °C (when using stored LCH, ensure that it equilibrates to room temperature and the pH is correct before use).
2. Assemble the following equipment prior to collection of tissue to ensure rapid microdissection of the retinas: serrated forceps, curved scissors, dissection dish (silicone-coated Petri dish), single edged blade, 2 sets of forceps (blunt) 1 glass Pasteur pipette (fire polished to a smooth but not narrow tip), 1 disposable plastic pipette (with tip trimmed off to increase the aperture to ~ 5 - 7 mm), 1 glass round bottom test tube (5 mL) and holder. Decant approximately 50 mL of LCH into a glass beaker and prepare a second beaker to decant waste fluids.
    NOTE: See **Table of Materials** for specifications and manufacturer details.
3. Euthanize the rat using CO_2 followed by cardiac puncture to exsanguinate (avoid cervical dislocation or concussion as these may damage blood vessels in the eye). Retract the eyelids with serrated forceps, then use the curved scissors to cut around the orbital muscles and through the optic nerve. Gently extract the eyes from the orbit taking care to cut through any remaining attachments with scissors.
4. Place the eyes immersed in LCH solution on the dissection dish (eyes can be transported on ice in a solution of LCH if necessary). Use one set of blunt forceps to anchor the eye to the dish by holding the orbital muscle attachments or optic nerve; ensure that the anchoring point is as close as possible to the sclera to stabilize the eye.
5. Using the blade, cut through the cornea along the *ora serrata* and remove the lens by pressing gently on the sclera with forceps.
6. Cut the eye cup in half symmetrically through the optic disc. Using closed forceps gently 'brush' out the retinas from the two halves of the eyecup taking care to remove any remaining attachments at the optic disc. Repeat the process with the second eye and transfer the dissected retinas into the test-tube using the plastic pipette and a small drop of LCH medium.
7. Using the plastic pipette fill the test tube with LCH to ~ 5 mL and allow the retinas to settle to the bottom.
8. Wash the tissue approximately 3 times by removing ~ 4 mL of solution from the tube and adding fresh LCH using the plastic pipette. Where necessary, remove extraneous tissue such as suspensory ligaments, vitreous humor and hairs.
9. Wash the inside of the glass Pasteur pipette (polished tip) with LCH to prevent the tissue from sticking to the pipette. Using the same pipette, remove approximately 4 mL of solution from the test-tube. Then add approximately 2 mL of fresh LCH.
10. Gently dissociate (triturate) the retinas by drawing the tissue through the tip of the glass pipette slowly and expel the contents into the test-tube. Note, try not to introduce bubbles at this stage.
11. Repeat step 1.10 until the retinas are broken up to a size of approximately 2 - 3 mm^2.
12. Wash the inside of the pipette with approximately 2 mL of LCH and expel this into the test-tube. Allow the contents to settle to the bottom over 5 - 10 min.
13. Repeat the trituration process as outlined in 1.10 - 1.12 with a little more force until the tissue pieces are approximately 1 mm^2 in size. Again, allow the tissue to settle for 5 - 10 min.
14. Repeat steps 1.10 - 1.12 a third time with more force until the contents are fully homogenized and no pieces of retina remain (the solution should become milky in appearance).
    NOTE: This technique will yield up to 8 arteriolare segments (relatively free of surrounding neuropile and with some branches remaining intact) per isolation measuring 8 - 45 µm in diameter and 200 - 2500 µm in length.
15. Transfer a small quantity of the isolate into a physiological recording chamber or add fluorescent dyes for measurement of intracellular Ca^{2+} concentration ($[Ca^{2+}]_i$; see section 3). Dispose of remnants of eye cups and solution removed during the isolation process in accordance with local rules on handling of animal waste.
    NOTE: While it is advisable to experiment on vessels immediately after isolation, surplus isolate can be stored at 4 °C for up to 8 h.

2. Arteriolar Pressure Myography

NOTE: Arteriolar pressure myography is carried out as follows using equipment detailed in **Figure 1A**, **B** and the **Table of Materials**.

1. Transfer an aliquot of retinal vessel homogenate (1 - 2 mL; isolated as per section 1) to a physiological recording chamber (partially filled with nominally Ca^{2+}free Hanks' solution; $0Ca^{2+}$ Hanks'; see **Table 1**) mounted on the stage of an inverted microscope. Leave the vessels to settle on the bottom of the recording chamber for at least 5 min prior to experimentation.
2. Visually scan across the recording chamber to identify arterioles > 200 µm in length and possessing an open end through which the vessel can be cannulated (identification of vessel type is further explored in the results section). Position the vessel in the center of the field of view. If no suitable vessels are present, transfer another aliquot of vessel homogenate into the recording chamber as per step 2.1.
3. Anchor one end of the vessel using fine forceps and a small tungsten wire slip (75 µm diameter and ~ 2 - 4 mm in length) placed over the vessel (see **Figure 1C**(i)). To do this hold the wire in the forceps and locate the forceps above the recording chamber.
    1. Identify the corresponding shadow of the forceps under the microscope, lower the forceps into the bath until the wire becomes apparent. Position the wire over the vessel approximately 200 µm from the open end and drop the wire perpendicular to the long axis of the vessel.

NOTE: The weight of the tungsten wire is sufficient to occlude the vessel distally stopping flow of luminal contents during cannulation and pressurization.

4. Move the arteriole into a suitable position within the recording chamber such that it lies horizontally across the bath with the open end in line with the pressurization cannula (see **Figure 1C**(ii-iv)). Do this by gently nudging the occluding tungsten wire slip with an additional section of wire held within the forceps; do not touch the arteriole as it will irreversibly adhere to the forceps.

5. Where necessary (for long arteriole segments), add additional tungsten wire slips over the vessel such that the distance between the occluded and open ends of the vessel is no more than 200 µm; this helps to prevent the arteriole moving out of the field of view upon pressurization. If the vessel has any side branches, these should also be occluded with additional tungsten wire slips. If a side branch cannot be occluded discard the vessel.

6. Perfuse the chamber with $0Ca^{2+}$ Hanks' at 37 °C to remove extraneous retinal tissue and to warm the bath to physiological temperatures.
   NOTE: A standard gravity-fed bath perfusion and in-line heater system can be used for this purpose (see **Figure 1A**). $0Ca^{2+}$ Hanks' is used to facilitate the cannulation procedure, since removal of external Ca^{2+} ensures that the arterioles remain dilated.

7. Fabricate pressurization cannulas from filamented borosilicate glass capillaries (tip diameter ~3 - 10 µm depending on the diameter of the vessel to be cannulated; smaller vessels require narrower cannulas; see the **Table of Materials**) using a microelectrode puller and back-fill with $0Ca^{2+}$ Hanks' solution. Ensure the shank of the cannula is tapered gently towards the tip to facilitate cannulation.

8. Mount the cannula in a pipette holder attached to a 10 mL syringe via a Y-connector and a 3-way tap; this is used to pressurize the system, pressure being recorded using a manometer attached to the other side-arm of the Y-connector (see **Figure 1B**).
   NOTE: A 'helper' pipette is required to assist with the cannulation process. Fabricate the pipette from a borosilicate glass capillary pulled on a microelectrode puller to a tip diameter of 0.5 - 2 µm. Heavily fire polish the pipette (often until closed) using a microforge.

9. Carefully position the helper pipette at right angles to the long-axis of the vessel close to the open end using a 3-axis mechanical manipulator (see **Figure 1D**). Position the helper pipette just above the vessel, but not touching it.

10. Position the cannulation pipette at the open end of the vessel (see **Figure 1D** and **2A**(i)) using a fine micromanipulator; position the tip immediately adjacent to the opening, as assessed by adjusting the plane of focus on the microscope (at 20X). When both the end of the vessel and the cannula tip are in focus at the same time the cannula is correctly positioned for cannulation (see **Figure 2A**(ii)).

11. Advance the pressurization cannula into the vessel aperture using the x-axis controls of the fine micromanipulator (see **Figure 2A**(iii)). Assess the success of cannulation by moving the cannula along the y-axis. If the cannula remains within the vessel it is successfully cannulated (see **Figure 2A**(iv)). If the cannula moves outside of the vessel, the cannula is likely to be above the vessel; if so repeat step 2.10 - 2.11 with the cannula at a lower plane in the z-axis.

12. Upon successful cannulation gently lower the helper pipette onto the vessel to restrain the arteriole. Guide the arteriolar wall over the pressurization cannula with the helper pipette, at the same time as the cannulation pipette is advanced further into vessel lumen to a distance of approximately 30 - 50 µm (see **Figure 2A**(v,vi)).
    NOTE: This procedure requires simultaneous, controlled movement of both manipulators (helper pipette moving towards the cannula while the cannula moves into the vessel lumen) and will require extensive practice to achieve a high success rate.

13. Change the bath solution to normal Hanks' containing 2 mM Ca^{2+} (see **Table 1**) at 37 °C. Typically this causes a slight narrowing of the arteriole and the formation of a tight seal around the pressurization cannula. The helper pipette can then be moved away from the vessel.

14. Allow a tight seal to develop for 15 min. View the vessel using a USB camera (and image acquisition software) attached to the microscope and adjust the focus to maximize the contrast between the vessel boundaries and the external and intraluminal spaces (see **Figure 2B**). Image the vessel at 0.5 - 5 frames/s.

15. After 1 min of recording at 0 mmHg, increase the intraluminal pressure to the desired level by closing the 3-way tap attached to the pressurization cannula (see **Figure 1B**) and apply a small amount of positive pressure to the system via the syringe. Observe the pressure change on the manometer.
    NOTE: Pressure can be added in a step wise fashion up to 100 mmHg or to one value for example 40 mmHg (approximating retinal arteriolar pressure *in vivo*)[23]. The vessel should rapidly dilate confirming successful cannulation. Please note, pressure-induced vasoconstriction (*i.e,* the myogenic response) will subsequently develop over a period of 15 min, but because of the small size of these vessels, this may not always be visually detectable.

16. Carefully monitor the vessel during initial pressurization for obvious leaks. Sources of leak may originate from cleaved side branches or inadequate sealing of the cannula to the inside of the arteriole.
    1. Watch for intraluminal contents leaving the vessel. Smaller, less obvious leaks may become apparent over time as a drop in pressure on the manometer. If possible, occlude the opening with additional tungsten wire slips taking care not to disturb the cannula. Exclude preparations with obvious leakage from further analysis.

17. Apply the drug of interest abluminally to the vessel prior to, or following, 15 min pressurization depending on the aims of the experiment (the former allows effects on the development of the myogenic tone to be determined, while the latter enables analysis of effects on steady-state myogenic tone). A typical drug delivery system is pictured in **Figure 3A**.
    1. Position the delivery outlet perpendicular to the portion of vessel of interest (as illustrated in **Figure 1D**) at a distance ~ 500 µm away from the vessel of interest taking care to ensure that the outlet is optimally angled to fully superfuse the area (see **Figure 3B**). Ensure that changes in perfusion do not physically disturb the vessel.

18. Following completion of an experiment, apply a solution of $0Ca^{2+}$ Hanks' containing 10 µM wortmannin (myosin light chain kinase inhibitor) to maximally dilate the vessel to determine the passive diameter.
    NOTE: The strength of the cannulation seal can be tested at the conclusion of the experiment by raising the intraluminal pressure to >100 mmHg. The majority of vessels will remain attached even at this high pressure indicating a tight seal.

19. Perform offline analysis using edge detection to track changes in the arteriolar diameter (see **Table of Materials** for suggested software). Normalize the arteriole diameter to the passive diameter for comparison between vessels.

3. Ca^{2+} Imaging

Note: Isolated retinal arterioles are prepared for conventional (microfluorimetry) and confocal Ca^{2+} imaging as follows (using equipment detailed in **Table of Materials**).

1. Prepare retinal homogenates in a 5 mL glass test tube as described in section 1. To 1 mL of retinal homogenate add Fura-2AM (microfluormetric Ca^{2+} recording) or Fluo-4AM (confocal Ca^{2+} imaging) to give a final concentration of 5 µM (protect from light); dye indicators preferentially load into smooth muscle cells.
2. Maintain at room temperature in the dark for 2 h flicking the side of the tube every 15 - 20 min to re-suspend the retinal tissue. Thereafter, dilute the homogenate 1:4 with LCH solution to reduce further dye loading.
   NOTE: Vessels remain viable for up to 6 h (when stored at 4 °C and in the dark); however it is recommended that experiments are commenced as soon as possible to reduce the impact of compartmentalization of the dye in internal organelles or extrusion of the dye over time.
3. Transfer 1 - 2 mL of retinal homogenate to a glass-bottomed recording chamber (partially filled with LCH) mounted on the stage of an inverted microscope connected to a Ca^{2+} microfluorimetry or confocal microscopy system.
   1. Anchor arterioles perpendicular to the direction of flow across the recording chamber, with tungsten wire slips (50 µm diameter, 2 - 4 mm in length) spaced ~ 100 - 200 µm apart along the vessel length (see **Figure 3C**) using a similar technique to that described in step 2.3.
4. Perfuse the bath with normal Ca^{2+} Hanks' solution at 37 °C. Position the drug delivery outlet as pictured in **Figure 3C** and apply drugs to vessels as described in step 2.17.
5. For conventional Ca^{2+} imaging, illuminate the vessel with 340/380 nm light via an oil immersion UV objective (*e.g.,* 100X, NA 1.3) and collect emitted fluorescence at 510 nm via a photon counting photomultiplier tube (PMT).
6. At the end of each experiment, measure background fluorescence by quenching the vessel with a MnCl-containing solution (see **Table 1**). Use background-corrected fluorescence ratios (R-F340/F380) for analysis or convert to intracellular Ca^{2+} ([Ca^{2+}]$_i$) using R_{min} and R_{max} measurements (see Table 1; applied prior to quenching[24]) and the Grynkiewicz equation[25].
7. For confocal Ca^{2+} imaging, excite Fluo-4 loaded vessels at 488 nm and capture the resultant fluorescence emissions at 490 - 535 nm in either line scan mode (xt) or xyt scan modes (512 x 512 pixels; suggested pinhole 300 nm). Normalize measurements to the fluorescence recorded at time t=0s (F/F$_0$). Assess any changes in [Ca^{2+}]$_i$ during drug applications or pressurization offline in specific regions of interest (ROIs) using image analysis software.
8. If needed, perform Ca^{2+} imaging with pressure myography.
   NOTE: The descriptions above have been optimized for unpressurized vessels; however it is possible to combine Ca^{2+} imaging with pressure myography as follows.
   1. Isolate arterioles as per section 1. Load with Ca^{2+} indicator dyes as per step 3.1 - 3.2. Transfer the arterioles to the recording chamber and cannulate as per section 2. Take care to limit exposure to light during the mounting procedure.
   2. Measure Ca^{2+} as per step 3.5 or 3.7 above. Pressurize the vessel and repeat the measurement of Ca^{2+}. Simultaneous measurement of vessel diameter is dependent on the mode of Ca^{2+} measurement and equipment used.
      NOTE: For confocal Ca^{2+} measurement it may be necessary to image separate regions pre- and post- pressurization due to bleaching of the dye during long exposures to light.

4. Patch-Clamp Electrophysiology

Note: Whole-cell and single-channel recording is possible from individual arteriolar smooth muscle cells still embedded within their parent arterioles as follows (using equipment detailed in **Table of Materials**).

1. Isolate and anchor retinal arterioles in the recording chamber as described in steps 1, 2.3, and 3.3. For patch-clamp recording, the tungsten wire slips are spaced 200 - 800 µm apart along the vessel.
2. Remove basal lamina surrounding the arteriole and electrically uncouple adjacent smooth muscle cells and underlying endothelial cells prior to patch clamping. To do this, superfuse the vessel with a sequential series of enzyme solutions (**Table 1**) at 37 °C for the required duration.
   NOTE: The duration of enzyme exposure is optimized for rat retinal arterioles (protease, ~ 8 min; collagenase, ~ 12 min) and depends on the flow rate of the drug delivery system (~1 mL/min on our set-up) and the unit activities of the batch of enzymes being used.
3. Evaluate the level of digestion on visual separation of endothelial and smooth muscle layers during the collagenase step as shown in **Figure 4**. Once separation of the cell layers is observed (as shown in **Figure 4B**), apply DNAse I solution (~ 4 min) then terminate the digestion by replacement of the bath solution with normal Ca^{2+} Hanks' solution.
4. Remove any remaining strands of basal lamina and/or peripheral neuropile by carefully sweeping the closed tips of fine forceps along the surface of the vessel.
5. Pull and polish glass capillaries (**Table of Materials**), fill with pipette solution (**Table 1**) and place securely in the pipette holder of the patch-clamp headstage. Position the pipette at a 45° angle in relation to the recording chamber and advance it towards the vessel using the coarse setting on a motorized micromanipulator.
6. Select a smooth muscle cell protruding from the vessel wall and whose surface is free from visible debris (see **Figure 4B**). Position the tip of the patch pipette vertically over the cell of interest and lower gradually using the fine/slow movement of the micromanipulator to make contact with the smooth muscle membrane.
   1. Assess the contact between cell and pipette visually from cell movement and a change in the pipette resistance measured using the membrane (seal) test protocol in the acquisition software (5-10 mV negative step from 0 mV, frequency 25 KHz; see **Figure 5A**(i)).
7. When the seal resistance has increased 5-fold (*e.g.,* rising from 2 to 10 MΩ; **Figure 5A**(ii)) apply negative pressure transiently to the back of the pipette holder via a y-connector, 3-way tap, syringe and tubing attached to the pipette holder (assembled in a similar manner to that used in pressurization of arterioles, see **Figure 1B**).

8. Repeat applications of negative pressure until a gigaseal (>1 GΩ resistance; as indicated by the membrane test in the acquisition software) is formed (**Figure 5A**(iii)). Note, this process may take 1 - 5 min. If a gigaseal fails to form, choose a different cell to patch clamp using a fresh patch pipette.

9. Apply a holding potential to the cell via the acquisition software as per the experiment being performed (typically 0, -40 or -80 mV).

10. Study (on-cell) single channel activity in the present configuration. Alternatively, generate inside-out patches by rapidly retracting the patch pipette from the cell surface after gigaseal formation.
    1. As the free ends of the membrane can re-anneal under these conditions remove the pipette from the bath via rapid vertical movement of the manipulator (coarse setting). Rapidly return through the meniscus to remove the reformed membrane leaving only the patch inside the pipette tip.

11. Set the sampling frequency on the acquisition software to 5 KHz and activate continuous recording mode to record channel activity. Apply any voltages changes if required via the software or the amplifier.

12. If required, apply drugs to vessel/membrane patch as described in step 2.17.

13. If membrane stretch is required, apply negative pressure to the posterior of the pipette using the syringe attached to a manometer via a 3-way tap and y-connector.

14. Analyze single channel recordings for open probability and unitary conductance in accordance with standard procedures[26].

15. For whole cell current recording pull and polish pipettes as per the **Table of Materials**, fill with pipette solution containing amphotericin B (add 3 mg of amphotericin B to 50 µL of DMSO; add 3-6 µL of this to 1 mL of whole-cell pipette solution; sonicate to mix) and form a seal as per steps 4.6 - 4.9.

16. Due to the inclusion of amphotericin B there is no need to rupture the membrane within the pipette tip to gain whole cell access. Monitor access, which will be gained gradually, using the membrane test protocol in the acquisition software (-20 mV step from -40 mV, sample frequency 25 KHz; see **Figure 5B**).

17. Automated fitting of capacitive transients in some software yields real-time measurements of access resistance and cell capacitance (alternatively the relative decline of the transients can be assessed by eye). Once the access resistance falls to < 15 MΩ, perform series resistance compensations (**Figure 5C**) using the whole-cell parameter dials (capacitance and series resistance) on the amplifier.
    1. To do this, use the automated fitting values to initially set the dials (see **Figure 5C**(ii)) then increase the series resistance compensation dial (both prediction and correction if available on the amplifier) re-adjusting the whole cell compensations while reducing the capacitive transient (see **Figure 5C**(iii)).
    2. Taking care not to over compensate (as shown in **Figure 5C**(iv)). Typically, it is possible to compensate the series resistance by 75% in perforated patch mode (requires lag compensation to be set at maximum).

18. If no automated fitting is available, start by setting the whole-cell parameters dials to 15 pF and 15 mΩ (typical values for these cells) and then adjust to produce the outputs as shown in **Figure 5C**(ii). Increase the series resistance compensation dial to ~75% and readjust the whole-cell parameters dials as per **Figure 5C**(iii).

19. Prior to commencing experimentation note the cell capacitance measurement either from the initial automated fitting or from the dial after manual compensation.
    NOTE: This value is used to normalize currents to cell size. Compensation for series resistance may need to be adjusted during experimentation as access may continue to improve due to further incorporation of amphotericin B into the patch.

20. Apply drugs to vessels as described in step 2.17. Apply voltage protocols (either steps or ramps) as per experimental requirements.
    NOTE: Typical voltage step protocols, 0.1 - 1 s in duration, are applied from the holding potential in 10 - 20 mV increments every 5 - 10 s to produce a family of voltage-activated currents. Alternatively use ramp protocols to measure currents at a series of voltages in one 'sweep' by ramping the voltage slowly (100 - 200 mV/s) from *e.g.,* -80 to +80 mV (applied every 5-10 s) with offline sampling of the current at 10 mV intervals during the ramp.

21. It is possible to combine Ca^{2+} imaging with patch-clamp recording as follows. Isolate arterioles as per section 1. Load with Ca^{2+} indicator dyes as per steps 3.1 - 3.2. Mount in the recording chamber as per section 4. Take care to limit exposure to light during these procedures.
    NOTE: To date it has not been possible to combine patch-clamp with pressure myography studies due to the loss of the basement membrane and vessel integrity during the enzymatic dissociation process

Representative Results

Figure 6A shows a schematic drawing of the rat retinal vascular tree. The diameter ranges of the first order (30 - 45 µm), second order (20 - 30 µm), and pre-capillary arterioles (8 - 20 µm) has been confirmed experimentally in our laboratory by confocal imaging of rat retinal whole-mount preparations immunohistochemically labelled for α-smooth muscle actin (**Figure 6B**). Upon dissociation of the retina, primary, secondary and pre-capillary arterioles can be identified based on their caliber and the arrangement of the vascular smooth muscle cells. The first and second order arterioles appear visually similar under bright-field microscopy, but can be distinguished on the basis of their size (**Figure 6C**). The pre-capillary arterioles are the smallest arterial vessels in the preparation and are easily recognizable due to their sparser arrangement of vascular smooth muscle fibers. The isolated arterioles can be clearly differentiated from capillaries and venules within the isolation. Capillaries are apparent as a meshwork of small caliber (4 - 10 µm in diameter) vessels, while venules are thin walled and lack smooth muscle cell coverage (**Figure 6C**). Primary, secondary and pre-capillary arterioles are suitable for pressure myography, Ca^{2+} imaging and patch-clamp studies.

Figure 7 shows a pressure myography experiment where a primary rat retinal arteriole has been cannulated and the intraluminal pressure raised to 40 mmHg. The arteriole is then maintained at this pressure to allow for the development of myogenic tone prior to the addition of $0Ca^{2+}$ Hanks' containing 10 µM wortmannin to obtain the passive diameter of the vessel. **Figure 7A** shows photomicrographs of the arteriole at various time points during the course of the experiment. A full time-course record showing the changes in vessel diameter over time have been plotted in **Figure 7B** using custom made edge-detection software[27]. Immediately upon pressurization the vessel dilates, which is then followed by an active myogenic constriction that reaches a steady-state level after 15 min. Addition of $0Ca^{2+}$ Hanks'/wortmannin solution dilates the vessel back to a level similar to that observed immediately following the initial pressure step. As described above, drugs may be applied to the vessels before or following pressurization to investigate the mechanisms underlying the development and maintenance of myogenic tone in these vessels. Using this approach, we have previously shown that stretch-activated Transient Receptor Potential Vanilloid 2 (TRPV2) channels and L- and T-type voltage-gated Ca^{2+} channels play a central role in facilitating myogenic tone development in first and second order rat retinal arterioles[20,21,22]. We have also reported that large-conductance Ca^{2+} activated potassium channels (BK channels)[19,28] and K_v1-containing voltage-gated K^+ channels act to oppose myogenic activity in these vessels, since addition of specific inhibitors for each of these channels triggers vasoconstriction (**Figure 7C**).

Figure 8 shows examples of conventional and confocal Ca^{2+} imaging in retinal arterioles prior to and following exposure to the vasoconstrictor peptide, endothelin-1 (Et-1). In conventional fura-2-based recordings (**Figure 8A**), Et-1 (10 nM) elicits a biphasic increase in $[Ca^{2+}]_i$ in the retinal arteriolar smooth muscle layer, comprising of an initial transient component followed by a lower sustained component. We have previously characterized the transient and sustained components as being due to Ca^{2+} release from the endoplasmic reticulum and Ca^{2+} influx from the extracellular space, respectively[29]. Fluo-4-based confocal Ca^{2+} imaging provides a more detailed picture of the effects of Et-1 at the cellular level. In these experiments, it is evident that the smooth graded changes in global $[Ca^{2+}]_i$ observed in our microfluorimetry studies result from Et-1 stimulating the activation of repetitive asynchronous $[Ca^{2+}]_i$ oscillations in the neighbouring retinal arteriolar smooth muscle cells along the vessel wall (**Figure 8B**, **C**;[30]).

Figure 9 shows examples of single-channel and whole-cell patch clamp recordings from retinal arteriolar smooth muscle cells. To date, we have carried out both on-cell and inside-out single channel patch clamp recordings[22,28]. **Figure 9A**, B for example, show an on-cell patch clamp recording prior to and following membrane stretch (generated by applying negative pressure to the patch pipette). This particular patch contains two channels which are activated by mechanical stretch. We have previously demonstrated that these currents can be inhibited using TRPV2 channel pore-blocking antibodies[22]. The unitary conductance of the channels (249.71 pS) is also consistent with these currents being mediated by TRPV2[31].

Whole-cell voltage-activated currents can be evoked using voltage step protocols. **Figure 9C** shows a family of voltage-activated A-type K^+ currents recorded using such an approach. These currents become evident when other large currents present in these cells (*e.g.,* BK and Ca^+-activated Cl^- currents) are blocked using specific pharmacological agents[32,33]. Currents through non- or weakly voltage-dependent ion channels are typically examined using voltage ramp protocols. We have used such protocols to identify and characterize TRPV2 currents activated by hypotonic stretch[22] and channel agonists (**Figure 9D**) in retinal arteriolar smooth muscle cells.

Figure 10 shows dual pressure myography and confocal Ca^{2+} imaging applied in a primary rat retinal arteriole. Pressurization triggers increased frequency of $[Ca^{2+}]_i$ oscillations in the individual smooth muscle cells similar to those observed with Et-1. We have previously shown that these oscillations are triggered by the summation of Ca^{2+} sparks (localized Ca^{2+} release events) and contribute to the generation of myogenic tone[20].
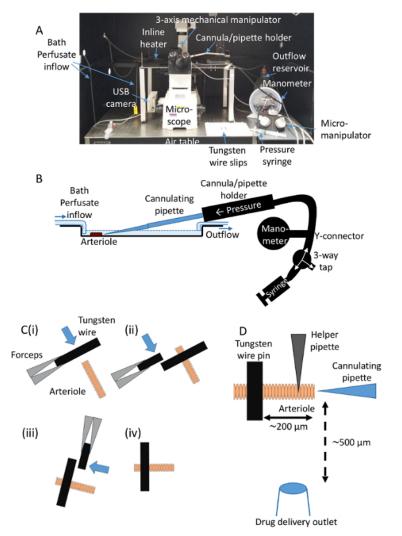
Figure 1. Experimental setup for pressure myography in rat retinal arterioles. A) Experimental equipment including inverted microscope, in-line heater for bath perfusate, 3-axis mechanical and micro-manipulators, manometer, cannula holder and air table. **B**) Schematic diagram showing the optimal arrangement of the cannulating pipette and vessel of interest in the recording chamber. This diagram also illustrates the basic set-up of the pressurization equipment. **C**) Schematic diagram shown the process of anchoring and moving the vessel using additional tungsten wire slips held in fine forceps. (i) Drop 1st slip to occlude vessel. (ii, iii) Use additional slips to nudge the occluding slip (direction indicated by the arrow) and accompanying vessel into the optimum orientation shown in (iv). **D**) Schematic diagram showing optimal positioning of occluding tungsten wire slip, helper pipette and cannula in relation to the vessel as arranged prior to cannulation. The outlet of the drug delivery system is positioned at a distance of ~ 500 µm from the vessel to reduce movement artifacts during drug application. Please click here to view a larger version of this figure.
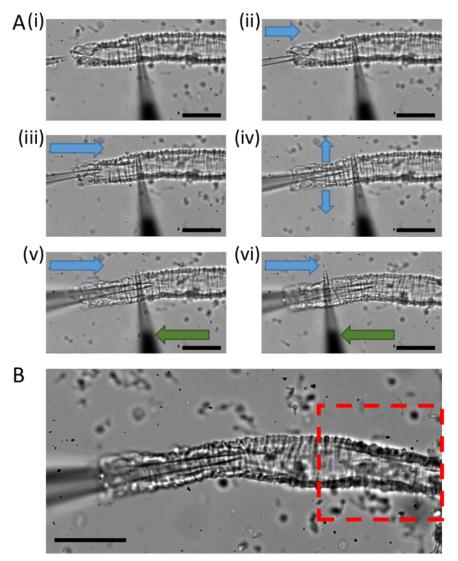
Figure 2. Cannulation process for pressure myography. A) Photomicrographs showing a retinal arteriole anchored down in the recording chamber prior to (i), during (ii)-(v) and following cannulation (vi). Blue arrow indicates direction of movement of the cannula while the green arrow indicates the direction of movement of the helper pipette. **B**) Photomicrograph showing optimal region for recording of myogenic activity during pressurization as highlighted in red. Note, adjustment of light and focus to increase contrast of vessel walls enables better tracking of vessels edges for automated analysis. Scale bar indicates 50 μm. Please click here to view a larger version of this figure.
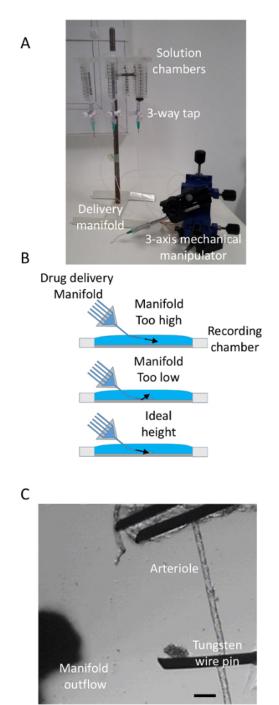
Figure 3. Drug delivery. A) Equipment used for drug delivery showing solution reservoirs connected to a multi-channel delivery manifold controlled by 3-way taps and attached to a 3-axis mechanical manipulator. **B)** Diagram showing the optimal vertical positioning of the drug delivery manifold in relation to the recording chamber. **C)** Photomicrograph of a vessel anchored down in the recording chamber showing the ideal positioning of the drug delivery outlet. Scale bar represents 100 µm. Please click here to view a larger version of this figure.
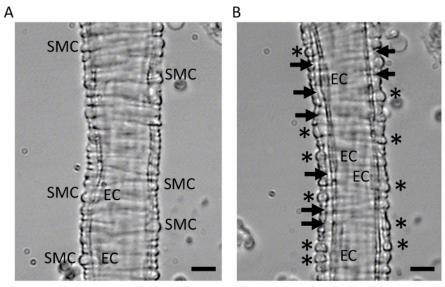
Figure 4. Enzymatic digestion of retinal arterioles for patch clamp recording. Light micrographs of a retinal arteriole before (**A**) and after (**B**) enzymatic digestion. Note the physical separation (indicated by arrows) of the smooth muscle cells (SMCs) from the underlying endothelial cells (ECs). Smooth muscle cells suitable for patch clamping are indicated with an asterisk. Scale bar represents 10 μm. Please click here to view a larger version of this figure.
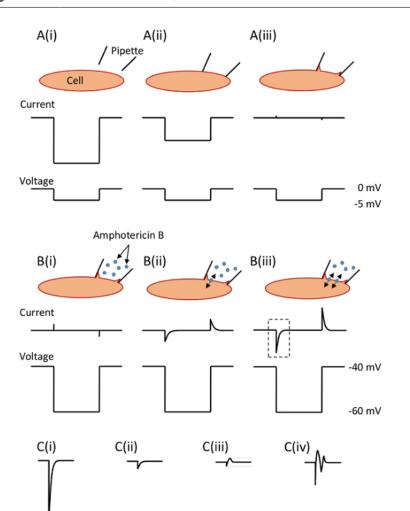
Figure 5. Single channel and whole cell patch clamp recording. A) Illustration of the test currents observed during the 'seal test' protocol when: (i) the patch pipette enters the external bathing medium, (ii) the pipette tip comes into contact with the vascular smooth muscle cell plasma membrane and (iii) suction is applied to the back of pipette to enable gigaseal formation. Following pipette capacitance compensation using the patch clamp amplifier, single channel currents may now be recorded in the on-cell configuration or a patch of membrane may be excised by rapidly withdrawing the pipette to create an 'inside-out' patch. **B**) Current changes associated with the development of electrical access to the cell interior during application of the amphotericin B whole-cell perforated patch clamp technique (i): (ii) As amphotericin B partitions into the membrane, access resistance falls and capacitance transients elicited during hyperpolarizing voltage steps (from -40 to -60 mV) become larger; (iii) once access resistance (R_a) has fallen to < 15 MΩ, which usually takes 5 - 10 min following gigaseal formation, experimentation is possible. **C**) Prior to whole-cell recording, access resistance and cell capacitance must be compensated using the relevant dials on the patch clamp amplifier. Values of access resistance and cell capacitance provided by automated functions within patch-clamp software can be used to help guide this process: (i) shows the capacitance transient prior to compensation taken from the highlighted region in B(iii); (ii) shows the reduction in the capacitance transient normally observed when the access resistance and capacitance are compensated; (iii) series resistance compensation should then be corrected up to 75% and access resistance and capacitance compensations fine-tuned such that the resulting transient should be relatively equal in amplitude above and below the plateau level of current during the step. (iv) Care should be taken to ensure that the access resistance is not over compensated (indicated by the presence of 'ringing' of the transient), which can occur sometimes if access continues to improve during the course of the experiment. Please click here to view a larger version of this figure.
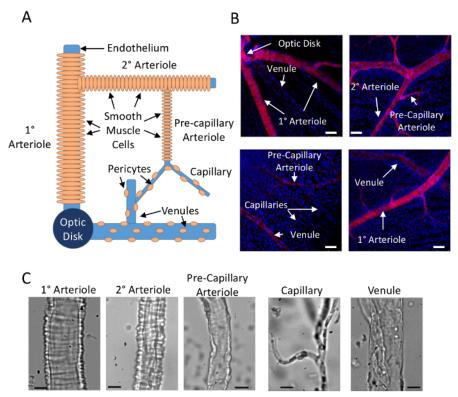
July 2018 | 137 | e57944 | Page 11 of 19

Figure 6. Identification of isolated rat retinal arterioles. **A**) Illustration showing the arrangement of the rat retinal microvascular tree. **B**) Confocal images of rat retinal arterioles and venules within flat mount preparations stained for αSMA (red; nuclei are stained blue; scale bars represent 50 μm). **C**) Light micrographs of isolated 1°, 2° and pre-capillary arterioles, a capillary network and venule (scale bars represent 10 μm). Please click here to view a larger version of this figure.
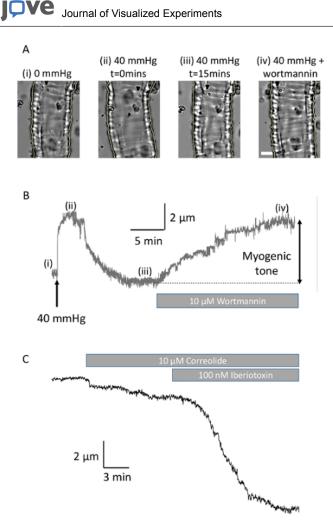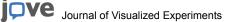
Figure 7. Arteriolar pressure myography recordings. **A**) Images of a cannulated retinal arteriole showing (i) resting diameter (approximately 35.6 μm), (ii) dilation upon pressurization, (iii) development of myogenic vasoconstriction and (iv) dilation due to the addition of 10 μM wortmannin in $0Ca^{2+}$ Hanks' solution. Scale bar represents 10 μm. **B**) Time course plot of the vessel diameter for the full experiment shown in A (sampled at 2.5 frames/s). **C**) Diameter trace from a different arteriole under steady-state myogenic tone (diameter 38.7 μm) showing the effects of the Kv1 channel inhibitor correolide (10 μM) and the BK channel inhibitor iberiotoxin (100 nM) (sampled at 0.5 frames/s). Please click here to view a larger version of this figure.
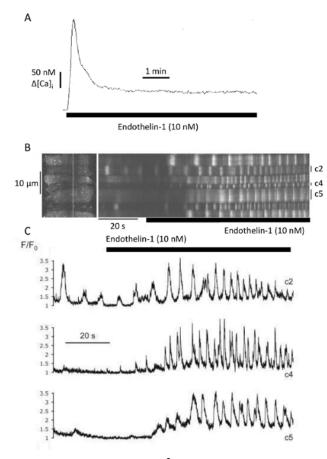
Figure 8. Effects of Et-1 on [Ca^{2+}]$_i$ signaling activity in rat retinal arterioles. **A**) Conventional fura-2-based recording showing the effects of Et-1 (10nM) on global [Ca^{2+}]$_i$. Basal [Ca^{2+}]$_i$ was 82 nM in this 1° arteriole. **B**) Fluo-4-based confocal xt images showing the effects of Et-1 on [Ca^{2+}]$_i$ at the cellular level. **C**) Plot of the normalized fluorescence intensity (F/F$_0$) measured in cells as marked in B. This figure has been modified from Tumelty et al.[30] with permission. Please click here to view a larger version of this figure.
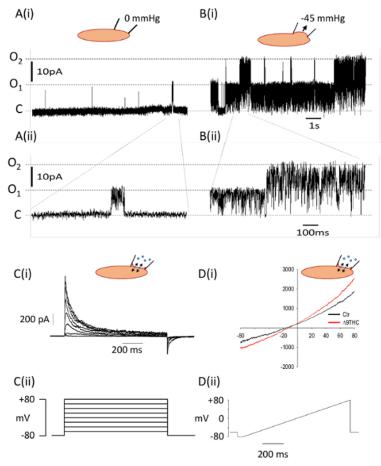
Figure 9. Single channel and whole-cell patch-clamp recordings from rat retinal arteriolar smooth muscle cells. **A**, **B**) On-cell single channel recordings from the same membrane patch prior to (A) and during (B) the application of negative pressure (-45 mmHg) to the patch pipette. Two channels are present in the patch (unitary current 12.81 pA; unitary conductance 249.71 pS) which show a substantial increase in activation under stretch conditions. Selected regions from the upper panels (i) are shown on a faster time base in the lower panels (ii). **C**) Family of A-type K^{+} channel currents (i) recorded in whole cell mode in the presence of inhibitors of BK and Ca^{2+}-activated Cl^{-} channel inhibitors, elicited in response to 20 mV voltage step increments between -80 mV to +80 mV (ii). **D**) Whole cell currents (i) elicited by voltage ramps between -80 mV and +80 mV before (black line) and during (red line) application of the TRPV2 channel agonist delta-9-tetrahydrocannabinol (Δ9-THC). The voltage ramp protocol used is shown in the lower panel (ii). Please click here to view a larger version of this figure.
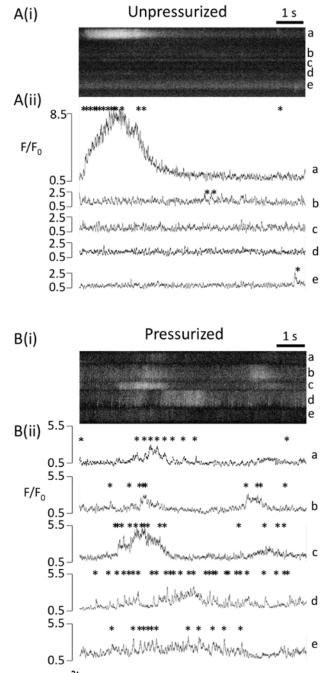
Figure 10. Ca^{2+} confocal imaging prior to and following pressurization of a rat retinal arteriole. Representative confocal xt scans (i) of retinal arteriolar smooth muscle cells under (**A**) unpressurized and (**B**) pressurized conditions obtained from separate regions of the same vessel. (ii) Changes in normalized fluorescence (F/F$_0$) recorded in individual cells a - e, as indicated in (i), plotted against time. Asterisks indicate individual subcellular Ca^{2+} sparks which increase in frequency after pressurization and summate to trigger cellular Ca^{2+} oscillations. Please click here to view a larger version of this figure.

Compound (mM)	Low Ca^{2+} Hanks'	0Ca^{2+} Hanks'	Normal Hanks'	Isolation enzyme Protease	Isolation enzyme Collagenase	Isolation enzyme DNAse	Quench solution	Rmin solution	Rmax solution	Cell attached Extracellular solution	Cell attached pipette solution	Whole-cell extracellular solution	Whole-cell pipette solution
Water purity (resistance)	≥15 MΩ.cm	≥15 MΩ.cm	≥15 MΩ.cm	≥15 MΩ.cm	≥15 MΩ.cm	≥15 MΩ.cm	≥15 MΩ.cm	≥15 MΩ.cm	≥15 MΩ.cm	≥15 MΩ.cm	≥18 MΩ.cm	≥15 MΩ.cm	≥18 MΩ.cm
NaCl	140	140	140	140	140	140	140	140	140			140	
kCl	6	6	6	6	6	6	6	6	6			6	138
D-Glucose	5	5	5	5	5	5	5	5	5	5	5	5	
MgCl$_2$	1.3	1.3	1.3	1.3	1.3	1.3	1.3	1.3	1.3	1.3	1.3	1.3	1
HEPES	10	10	10	10	10	10	10	10	10	10	10	10	10
CaCl$_2$	0.1		2	0.1	0.1	0.1			10	2	2	2	0.2
EGTA							4						0.5
MnCl							10						
Ionomycin									0.01				
KOH										140	130		
D-Gluconic acid										130	130		
NaOH											10		
Penitrem A										0.0001	0.0001	0.0001	
4-aminopyridine											10		
Nimodipine											0.01	0.01	
Fluoxetine											0.1		
9-anthracenecarboxylic acid												1	
Amphotericin B													300-600 µg mL^{-1}
Protease Type XIV				~0.01 % (0.4-0.6 mg/40 mL)									
Collagenase Type 1A					0.1 % (6 mg/60 mL)								
DNAse I						20 KU (20 µL of 1 MU/mL stock in 20 mL)							
pH	7.4	7.4	7.4	7.4	7.4	7.4	7.4	7.4	7.4	7.4	7.4	7.4	7.2
titrated with	NaOH	NaOH	NaOH	NaOH	NaOH	NaOH	NaOH	NaOH	NaOH	Tris	Tris	NaOH	KOH

Table 1. Composition of solutions used in experimentation including examples of external and pipette solutions used for single channel (TRPV2) and whole cell (A-Type) currents.

Discussion

The protocols described above require practice but should be achievable with minimal troubleshooting. On an average day we would obtain 6 - 8 usable arterioles from the isolation and achieve 3 - 4 successful experiments. If problems are encountered, however, there are some steps that can be taken to help improve success rates. Occasionally we have found, particularly when using younger rats (< 8 weeks), that the yield of arterioles can be low. To circumvent this problem, we would suggest centrifuging the retinal tissue (10 - 30 s at 500 x g) between each of the trituration steps in steps 1.12 - 1.14. This often helps to improve the yield of vessels but will also increase the amount of cell debris within the preparation.

When cannulating vessels for pressure myography studies it is important to check the arterioles carefully for any side-branches that may have been cleaved close to the bifurcation site. This represents a common cause of leakage and loss of pressure during experimentation. The main issue that can arise with the $[Ca^{2+}]_i$ protocols is the level of dye loading. Poor dye loading leads to low signal-to-noise ratios, while overloading results in disruption of normal Ca^{2+} homeostasis. To reduce the likelihood of either of these issues, a small aliquot of retinal homogenate can be removed, and isolated vessels checked periodically during the loading protocol. When undertaking patch-clamp experiments, the success rate of gigaseal formation is highly dependent on how well the basal lamina has been digested. When initially testing this protocol or using new lots of enzymes it may be necessary to adjust the concentration/duration of enzyme digestion. Carefully monitoring the separation of the endothelial and smooth muscle layers will ensure sufficient digestion to remove enough basal laminal to gain access. Careful monitoring is also necessary to avoid over-digestion, which can manifest as the vessel begins to constrict. If this occurs, the smooth muscle cells are often too fragile for patch clamp recording. When applying enzymes, it is important to include DNAse I to ensure removal of strands of DNA liberated from damaged cells during the isolation process. DNA fragments are sticky and cause the forceps to adhere to the arteriole during the final stages of the cleaning

process (step 4.4), often resulting in vessel loss. Cleaning of vessels is technically difficult and is best performed at high magnification (20X) with gentle sweeping motions of closed forceps of the finest possible tip diameter. Between sweeps, clean the forceps with lab roll.

As highlighted earlier, a key motivation behind the development of the protocols outlined in this manuscript was to better understand why blood flow is disrupted during retinal vascular diseases. Most of our work to date has focused on diabetic eye disease[28,33]. Arterioles can be isolated from the retinas of experimental rodent models of diabetes using the methods described in section 1. When experimenting on isolated retinal arterioles from diabetic animals, it is important to try to closely replicate the hyperglycemic conditions experienced by the vessels *in vivo*. For this reason, we would normally raise the D-glucose levels in our isolation and experimental solutions to 25 mM. Thickening of vascular basement membranes is a well-recognized phenomenon in retinal vessels during diabetes[34,35]. When using animals with prolonged diabetes (> 1 months disease duration), increased enzyme concentrations or digestion times are often needed to enable the application of patch-clamp recording methods.

An important limitation of using *ex vivo* isolated retinal arterioles to study retinal vascular physiology and pathophysiology is the loss of the surrounding retinal neuropile. Although removal of the retinal glial and neuronal cells enables easy access to the retinal vascular smooth muscle cells for cell physiology studies, the response of the vessels to vasoactive mediators can change dramatically in the absence and presence of retinal tissue. The actions of adenosine tri-phosphate (ATP), for example, provide a good illustration of this point. In isolated rat retinal arterioles, addition of ATP triggers a robust constriction of the vessels[36], while in the presence of an intact neuropile, the vessels dilate[37]. Therefore, wherever possible, we usually try to validate key findings from our isolated arteriole preparations using *ex vivo* retinal whole-mounts and *in vivo* measurements of vessel diameter and blood flow[16,37]. Of note, new methods have recently emerged for studying small arterioles and capillaries in whole perfused porcine retinas *ex vivo*[38,39]. Such preparations are likely to greatly improve our understanding of how the retinal neuropile regulates retinal arteriolar and capillary tone and how changes in retinal haemodynamics modulate neuronal activity in the retina.

Although the procedures described in this paper are focused on the use of isolated rat retinal arterioles for understanding arteriolar smooth muscle cell physiology, we are currently developing protocols to also enable the study of endothelial cell function in these vessels. In preliminary work, we have been successful in modifying the enzymatic digestion of retinal arteriolar segments to yield viable endothelial cell tubes that are amenable to Ca^{2+} imaging and patchclamp recording studies. Cannulation of the isolated arterioles at both ends, enabling intraluminal delivery of drugs, could in the future also enable endothelium-dependent vasodilatory responses to be investigated in these vessels.

Disclosures

Dr. Joanna Kur is now an employee of Medtronic (Twin-Cities, Minnesota, USA), her present work does not conflict with that presented here.

Acknowledgements

References

1. Kohner, E.M., Patel, V., Rassam, S.M. Role of blood flow and impaired autoregulation in the pathogenesis of diabetic retinopathy. *Diabetes.* **44,** 603-607 (1995).
2. Hafez, A.S., Bizzarro, R.L., Lesk, M.R. Evaluation of optic nerve head and peripapillary retinal blood flow in glaucoma patients, ocular hypertensives, and normal subjects. *American Journal of Ophthalmology.* **136,** 1022-31 (2003).
3. Curtis, T.M., Gardiner, T.A., Stitt, A.W. Microvascular lesions of diabetic retinopathy: clues towards understanding pathogenesis? *Eye (London).* **23,** 1496-1508 (2009).
4. Pournaras, C.J., Rungger-Brändle, E., Riva, C.E., Hardarson, S.H., Stefansson, E. Regulation of retinal blood flow in health and disease. *Progress in Retinal and Eye Research.* **27,** 284-330 (2008).
5. Kuwabara, T., Cogan, D.G. Studies of retinal vascular patterns. I. Normal architecture. *Archives of Ophthalmology.* **64,** 904-11 (1960).
6. Scholfield, C.N., McGeown, J.G., Curtis, T.M. Cellular physiology of retinal and choroidal arteriolar smooth muscle cells. *Microcirculation.* **14** (1), 11-24 (2007).
7. Puro, D.G. Retinovascular physiology and pathophysiology: new experimental approach/new insights. *Progress in Retinal and Eye Research.* **31** (3), 258-70 (2012).
8. Kur, J., Newman, E.A., Chan-Ling, T. Cellular and physiological mechanisms underlying blood flow regulation in the retina and choroid in health and disease. *Progress in Retinal and Eye Research.* **31** (5), 377-406 (2012).
9. Delaey, C., Van de Voorde, J. Regulatory Mechanisms in the Retinal and Choroidal Circulation. *Ophthalmic Research.* **32** (6), 249-56 (2000).
10. Metea, M.R., Newman, E.A. Glial cells dilate and constrict blood vessels: a mechanism of neurovascular coupling. *Journal of Neuroscience.* **26,** 2862-2870 (2006).
11. Pournaras, C.J., Rungger-Brändle, E., Riva, C.E., Hardarson, S.H., Stefansson, E. Regulation of retinal blood flow in health and disease. *Progress in Retinal and Eye Research.* **27** (3), 284-330 (2008).
12. Hughes, S., Chan-Ling, T. Characterization of smooth muscle cell and pericyte differentiation in the rat retina *in vivo*. *Investigative Ophthalmology & Visual Science.* **45** (8), 2795-806 (2004).
13. Shepro, D., Morel, N.M. Pericyte physiology. *The FASEB Journal.* **7** (11), 1031-8 (1993).
14. Kornfield, T.E. Newman, E.A. Regulation of Blood Flow in the Retinal Trilaminar Vascular Network. *Journal of Neuroscience.* **34** (34), 11504-11513 (2014).
15. Matsushita, K., Puro, D.G. Topographical heterogeneity of KIR currents in pericyte-containing microvessels of the rat retina: effect of diabetes. *Journal of Physiology.* **573,** 483-495 (2006).

July 2018 | 137 | e57944 | Page 18 of 19

16. Needham, M., *et al.* The role of K+ and Cl- channels in the regulation of retinal arteriolar tone and blood flow. *Investigative Ophthalmology & Visual Science.* **55** (4), 2157-65 (2014).

17. Hessellund, A., Jeppesen, P., Aalkjaer, C., Bek, T. Characterization of vasomotion in porcine retinal arterioles. *Acta Ophthalmologicaogica Scandinavica.* **81**, 278-282 (2003).

18. Delaey, C., Van de Voord, J. Pressure-induced myogenic responses in isolated bovine retinal arteries. *Investigative Ophthalmology & Visual Science.* **41,** 1871-1875 (2000).

19. Kur, J., *et al.* Role of ion channels and subcellular Ca^{2+} signaling in arachidonic acid-induced dilation of pressurized retinal arterioles. *Investigative Ophthalmology & Visual Science.* **55** (5), 2893-902 (2014).

20. Kur, J., Bankhead, P., Scholfield, C.N., Curtis, T.M., McGeown, J.G. Ca(2+) sparks promote myogenic tone in retinal arterioles. *British Journal of Pharmacology.* **168** (7), 1675-86 (2013).

21. Fernández, J.A., McGahon, M.K., McGeown, J.G., Curtis, T.M. CaV3.1 T-Type Ca^{2+} Channels Contribute to Myogenic Signaling in Rat Retinal Arterioles. *Investigative Ophthalmology & Visual Science.* **56** (9), 5125-32 (2015).

22. McGahon, M.K., *et al.* TRPV2 Channels Contribute to Stretch-Activated Cation Currents and Myogenic Constriction in Retinal Arterioles. *Investigative Ophthalmology & Visual Science.* **57** (13), 5637-5647 (2016).

23. Guidoboni, G., *et al.* Intraocular Pressure, Blood Pressure, and Retinal Blood Flow Autoregulation: A Mathematical Model to Clarify Their Relationship and Clinical Relevance. *Investigative Ophthalmology & Visual Science.* **55** (7), 4105-4118 (2014).

24. Scholfield, C.N., Curtis, T.M. Heterogeneity in cytosolic calcium regulation among different microvascular smooth muscle cells of the rat retina. *Microvascular Research.* **59** (2), 233-42 (2000).

25. Grynkiewicz, G., Poenie, M., Tsien, R.Y. A new generation of Ca^{2+} indicators with greatly improved fluorescence properties. *Journal of Biological Chemistry.* **260**, 3440-3450 (1985).

26. Sakmann, B., Neher, E. *Single Channel Recording, Second Edition.* 53-90 Plenum Press: New York, (1995).

27. Fernández, J.A., Bankhead, P., Zhou, H., McGeown, J.G., Curtis, T.M. Automated detection and measurement of isolated retinal arterioles by a combination of edge enhancement and cost analysis. *PLoS One.* **9**, e91791 (2014).

28. McGahon, M.K., *et al.* Diabetes downregulates large-conductance Ca^{2+}-activated potassium beta 1 channel subunit in retinal arteriolar smooth muscle. *Circulation Research.* **100** (5), 703-11 (2007).

29. Curtis, T.M., Scholfield, C.N. Nifedipine blocks Ca^{2+} store refilling through a pathway not involving L-type Ca^{2+} channels in rabbit arteriolar smooth muscle. *Journal of Physiology.* **532** (3), 609-23 (2001).

30. Tumelty, J., *et al.* Endothelin 1 stimulates Ca^{2+}-sparks and oscillations in retinal arteriolar myocytes via IP3R and RyR-dependent Ca^{2+} release. *Investigative Ophthalmology & Visual Science.* **52** (6), 3874-9 (2011).

31. Huynh, K.W., *et al.* Structural insight into the assembly of TRPV channels. *Structure.* **22** (2), 260-8 (2014).

32. McGahon, M.K., Dawicki, J.M., Scholfield, C.N., McGeown, J.G., Curtis, T.M. A-type potassium current in retinal arteriolar smooth muscle cells. *Investigative Ophthalmology & Visual Science.* **46** (9) **,** 3281-7 (2005).

33. McGahon, M.K., Zhang, X., Scholfield, C.N., Curtis, T.M., McGeown, J.G. Selective downregulation of the BKbeta1 subunit in diabetic arteriolar myocytes. *Channels (Austin).* **1** (3), 141-3 (2007).

34. Ljubimov, A.V., *et al.* Basement membrane abnormalities in human eyes with diabetic retinopathy. *Journal of Histochemistry and Cytochemistry.* **44,** 1469-1479 (1996).

35. Roy, S., Maiello, M., Lorenzi, M. Increased expression of basement membrane collagen in human diabetic retinopathy. *Journal of Clinical Investigation.* **93,** 438-442 (1994).

36. Scholfield, C.N., McGeown, J.G., Curtis, T.M. Cellular physiology of retinal and choroidal arteriolar smooth muscle cells. *Microcirculation.* **14** (1), 11-24 (2007).

37. Hinds, K., Monaghan, K.P., Frølund, B., McGeown, J.G., Curtis, T.M. GABAergic control of arteriolar diameter in the rat retina. *Investigative Ophthalmology & Visual Science.* **54** (10), 6798-805 (2013).

38. Torring, M.S., Aalkjaer, C., Bek, T. Constriction of porcine retinal arterioles induced by endothelin-1 and the thromboxane analogue U46619 *in vitro* decreases with increasing vascular branching level. *Acta Ophthalmologica.* **92** (3), 232-7 (2014).

39. Skov Jensen, P., Metz Mariendal Pedersen, S., Aalkjaer, C., Bek, T. The vasodilating effects of insulin and lactate are increased in precapillary arterioles in the porcine retina *ex vivo. Acta Ophthalmologica.* **94** (5), 454-62 (2016).